JOURNAL OF GEOPHYSICAL RESEARCH, VOL. 106, NO. C5, PAGES 9039–9055, MAY 15, 2001

How iceberg calving and grounding change the circulation and hydrography in the Filchner Ice Shelf–Ocean System

K. Grosfeld,[1] M. Schröder, E. Fahrbach, R. Gerdes, and A. Mackensen

Alfred Wegener Institute for Polar and Marine Research, Bremerhaven, Germany

Abstract. The formation of bottom water in the southern Weddell Sea is strongly influenced by the flow of Ice Shelf Water (ISW) out of the Filchner-Ronne Ice Shelf cavity. The breakout of three giant icebergs in 1986 and their grounding on the shallow Berkner Bank modified the circulation and water mass formation in the Filchner Trough and the adjacent sea areas. Hydrographic measurements along the Filchner Ice Shelf front, carried out with RV *Polarstern* in 1995, show significant changes in the water mass characteristics and flow patterns in the Filchner Trough in comparison to measurements from the early 1980s. Changes in the trough will affect the flow over the sill to the deep Weddell Abyssal Plain. We combine a three-dimensional ocean circulation model with conductivity-temperature-depth and stable isotope measurements to investigate the details of the circulation in front of and beneath the Filchner Ice Shelf. We assess the impact of stranded icebergs and a more southerly ice shelf front position caused by a 1986 iceberg calving event on the circulation and observed water mass properties. Results indicate variations of the flow pattern in the Filchner Trough and on Berkner Bank, where High-Salinity Shelf Water, the feedstock for ISW, is produced. The calving and grounding impacts illustrate the sensitivity of the ice shelf–ocean system to perturbations in local bathymetric settings.

1. Introduction

The Weddell Sea is known to be one of the major sources for cold and saline deep and bottom waters, which ventilate the abyssal global ocean [*Reid and Lynn*, 1971]. The primary source water mass advected from the northeast into the Weddell Sea is the Warm/Weddell Deep Water (WDW) with relatively high temperature and salinity [*Gordon*, 1971; *Foster and Carmack*, 1976; *Foldvik et al*., 1985a; *Schröder and Fahrbach*, 1999]. It is entrained in the upper ocean mixed layer where it loses heat and produces freshwater by sea ice melting. Precipitation and glacial ice that flows off the continent also contribute to the freshwater budget. However, the contribution of melting sea ice dominates this budget [*Harms et al*., 2001]. Part of the glacial ice flow feeds the floating ice shelves, which melt at their base. Another part of the continental freshwater enters the ocean over a much wider area through the melting of icebergs [*Jacobs et al*., 1992].

The flow of relatively warm water to and under the ice shelves determines the available heat to melt the ice. Regional density differences formed by freshwater and salt exchanges related to melting and freezing processes underneath an ice shelf drive a circulation in the subice cavity that is sometimes referred to as an ice pump process [*Robin*, 1979; *Lewis and Perkin*, 1986]. The coldest water is produced near deep grounding lines by the melting of glacial ice. Its subsequent rise along the ice shelf base yields supercooled water, which releases ice crystals that accumulate at the ice shelf base and form a "marine ice" layer. This term was introduced by *Oerter et al*. [1992] to differentiate the process and characteristics ice formed beneath ice shelves from those pertaining to sea ice and meteoric/glacial ice. Water with temperatures below the surface freezing temperature crosses the ice shelf front [*Lusquinos*, 1963] as Ice Shelf Water (ISW). The overflow of ISW at the continental shelf break and its subsequent mixing with WDW leads to deep and bottom water formation in the Weddell Sea [*Foldvik et al*., 1985a]. In addition to being an important ingredient for the bottom water formation process, ISW also contributes to shelf water modification. The sensitivity of shelf water formation to perturbations caused by iceberg calving is the subject of this study.

The southern Weddell Sea is bounded by the vast Filchner-Ronne Ice Shelf (Figure 1), which is the second largest ice shelf of Antarctica by area, comprising ~450,000 km^2 [*Fox and Cooper*, 1994]. From geophysical soundings and borehole measurements [*Engelhardt and Determann*, 1987; *Oerter et al*., 1992; *Thyssen et al*., 1992] a 14,400 km^3 marine ice layer was inferred to exist under ~100,000 km^2 of the central Ronne Ice Shelf [*Grosfeld*, 1993]. In the coastal zone of the Filchner Ice Shelf a second marine ice body of 150 m thickness extends over >4000 km^2 [*Grosfeld et al*., 1998]. Marine ice and the flow of ISW from the subice shelf cavity through the Ronne and Filchner Troughs [*Schenke et al*., 1998] are indicators of intensive ice shelf–ocean interactions.

Since the first complete hydrographic cross section along the Filchner-Ronne Ice Shelf front in 1979/1980 [*Gammelsrød and Slotsvik*, 1981], two main outflows of Ice Shelf Water have been regarded as sources for the formation of Weddell Sea Bottom Water, one in the Filchner Trough and one in the Ronne Trough [*Rohardt*, 1984; *Foldvik et al*., 1985a; *Gammelsrød et al*., 1994; *Schröder et al*., 1997]. Topographic conditions and water mass characteristics suggest the outflow from the Filchner

[1]Now at Institute for Geophysics, University of Münster, Münster, Germany.

Paper number 2000JC000601.
0148-0227/01/2000JC000601$09.00

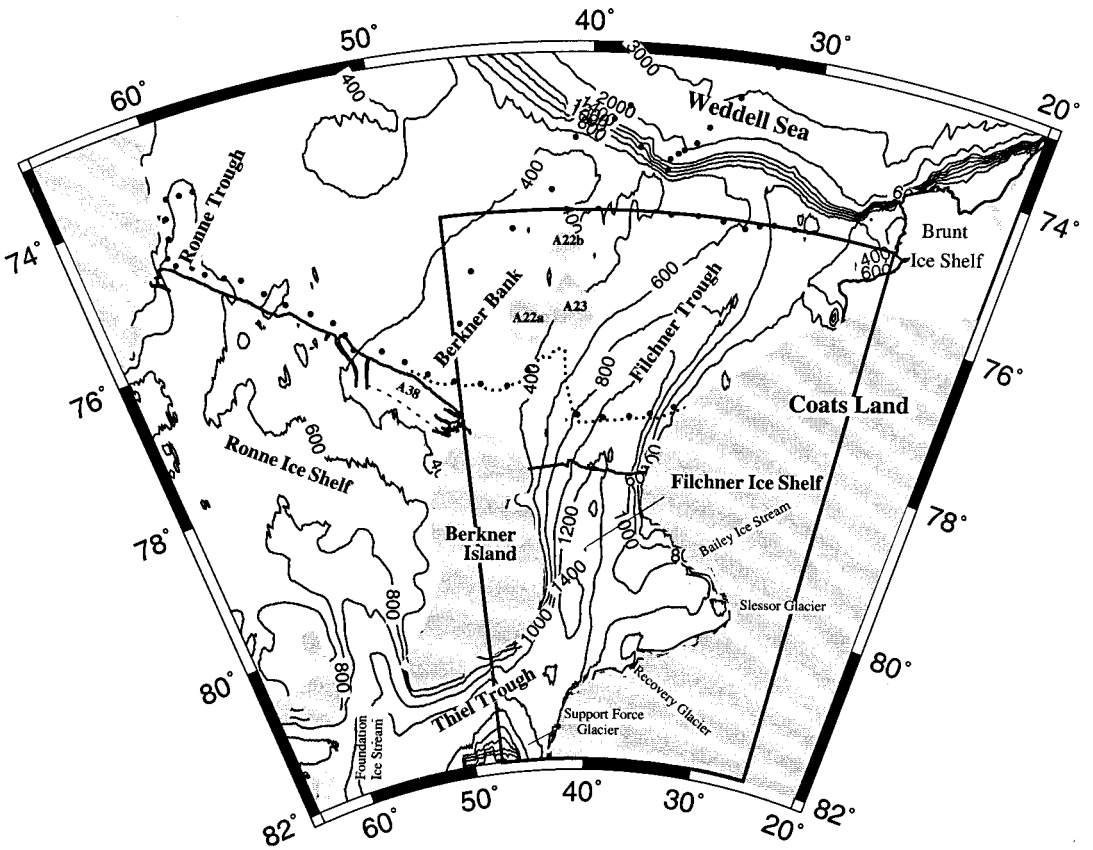

Figure 1. Map of the southern Weddell Sea showing the continental shelf, the grounded ice sheet (shaded area), and the Ronne and the Filchner Ice Shelves. The positions of grounded icebergs A22a, A22b, and A23 as observed in 1995 are indicated. The fast ice edge in front of the Filchner Ice Shelf is marked as dotted line. The contours give the bathymetry in meters. Conductivity-temperature-depth (CTD) stations measured during the RV *Polarstern* cruise ANT XII/3 are shown as dots. The area of iceberg A38, which calved from the Ronne Ice Shelf front in October 1998, is marked.

Trough is stronger [*Foldvik et al*., 1985a; *Foldvik and Gammelsrød*, 1988].

In August 1986, three giant icebergs (A22, A23, and A24), two ~3850 km^2 and one ~3000 km^2 in area, separated from the Filchner Ice Shelf front [*Ferrigno and Gould*, 1987] and grounded at the eastern Berkner Bank, fluctuating in position within the squares in Figure 2. With an average thickness of ~400 m their combined volume of ~4300 km^3 was roughly twice the annual accumulation over the Antarctic ice sheet [*Jacobs et al*., 1992]. In March of 1990, iceberg A24 came ungrounded and drifted northward through the Weddell and the Scotia Seas, disintegrating around 51°S, 47°W in April 1992 [*Vaughan*, 1993; *Grosfeld et al*., 1998]. Icebergs A22 and A23 broke in two in 1994 and 1991 with parts of each still grounded in the Filchner Trough.

This calving event and the subsequent groundings impacted the hydrographic structure in the Filchner Trough [*Gammelsrød et al*., 1994; *Nøst and Østerhus*, 1998], causing a pronounced change in the sea ice coverage and water mass characteristics. From an analysis of selected conductivity-temperature-depth (CTD) stations, *Nøst and Østerhus* [1998] concluded that prior to the calving, hydrographic conditions in the Filchner Trough were influenced by High-Salinity Shelf Water (HSSW) draining from its source region on Berkner Bank into the depression and by dense waters originating in front of the Ronne Ice Shelf entering the trough from south of Berkner Island. Only the coldest Ice Shelf Water in the medium 500–700 m depth range can be traced back to salinities of ~34.75, indicative of Ronne Ice Shelf waters, while other water masses with lower source salinity values originated on Berkner Bank.

When grounding occurred on Berkner Bank, conditions in the trough changed. In its deeper central and easterly parts, all waters changed their characteristics to those related to the Ronne Ice Shelf front. HSSW production on Berkner Bank now concentrated on the western side of the icebergs. Drainage of HSSW into the Filchner Trough had stopped, and Filchner Trough waters were only influenced by Ice Shelf Water from its remote source in front of Ronne Ice Shelf [*Nøst and Østerhus*, 1998, Figures 6d and 7d].

For this study we compare the 1980 and 1989 data sets from *Nøst and Østerhus* [1998] with the measurements from RV *Polarstern* in 1995. We only use the earlier data to extend our hydrographic data set prior to the calving event in 1986 and shortly thereafter for comparison with the model results. The 1984, 1987, and 1993 data presented by *Nøst and Østerhus* [1998] were taken at different locations and distances from the ice shelf front and therefore are not comparable to our measurements.

Here we used a numerical model to investigate the impact of the calving event on the regional flow pattern and the water mass formation in the Filchner Trough. After describing the

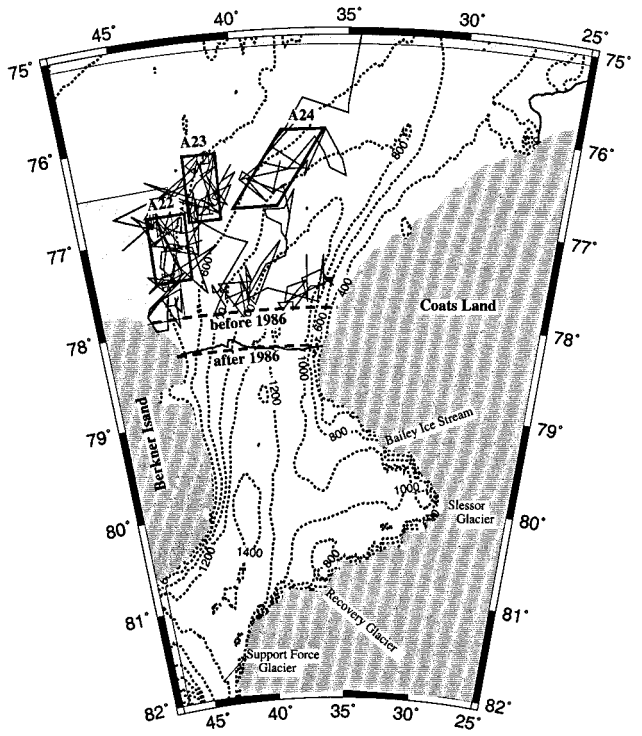

Figure 2. Physiographic map of the Filchner Ice Shelf model domain. The lines indicate the tracks of icebergs A22, A23, and A24 over the period 1986–1990, derived from National Ice Center charts (see http://www.natice.noaa.gov). The rectangles mark the mean position and adequate size of the icebergs over this period. In late 1989, A24 left the trough. Between 1990 and 1995, A22 and A23 shifted northward and broke into two parts each (see Figure 1). The position of the Filchner Ice Shelf front before and after the calving are shown as dashed lines. The light shaded areas along the open northern boundary, north and south of Berkner Island are restoring zones for tracer adjustment. Sea bottom depth (in m) is plotted as dotted lines.

model, we discuss the hydrographic structure found in 1995, 9 years after the calving event and 5 years after one iceberg (A24) had left the trough. The calving event and its impact on the circulation is simulated in three steps: (1) the precalving scenario before 1986, (2) the postcalving scenario, with all three icebergs in the trough on the eastern flank of Berkner Bank, and (3) the most recent (1995) scenario, where one iceberg had left the domain and only two icebergs remain grounded. With the model results as background we discuss the historical development of the calving event with temperature-salinity (Θ/S) diagrams of hydrographic measurements for the same periods and then summarize the impact on the water mass formation and the consequences for the overflow to the deep Weddell Sea.

2. Model Configuration

The Filchner Ice Shelf is separated from the Ronne Ice Shelf by Berkner Island (Figure 1). Only a channel (Thiel Trough) of ~120 km width connects the Filchner and the Ronne Ice Shelves in the south. The model area (box in Figure 1) extends from the southernmost part of Filchner Ice Shelf at 82°S to the northern limit of the Filchner Trough at ~75°S. In the west the domain is limited by the coastline of Berkner Island and a closed boundary along 47°30′W across the Thiel Trough south of Berkner Island and along the Berkner Bank. To the east the Coats Land coast limits the domain. For the model run representing the precalving scenario before 1986 the ice shelf front was located at 77.9°S. For those studies representing the postcalving scenario the ice shelf front was located at 78.3°S, and the icebergs were grounded on the Berkner Bank (Figure 2). Considering the grid spacing in the model, this corresponds to a calved area of ~9000 km^2, which is nearly the combined area A22, A23, and A24, i.e., 10,700 km^2. For the grounded icebergs an adequate size was chosen, covering the area of their mean residence on Berkner Island.

The ocean model is a version of a three-dimensional ocean general circulation model [*Bryan*, 1969; *Cox*, 1984], modified to use generalized vertical coordinates by *Gerdes* [1993]. This formulation has proven to be suitable for ice shelf cavity circulation problems because the seabed and the ice shelf base can be represented as coordinate surfaces. The introduction of a realistic ice front draft and coupling with the adjacent open ocean [*Grosfeld et al*., 1997] allows us to investigate the free interaction between both systems. For the present application we use a horizontal resolution of 0.3° by 0.1°, giving an approximate resolution of 4.6–8.6 km in longitude and 11 km in latitude. In the vertical plane, 10 layers beneath the ice shelf and 14 layers in the open ocean are used, varying from 2.4% of the water column thickness for the uppermost layers to ~25% for the bottom layer. The model configuration is similar to that described by *Grosfeld and Gerdes* [1998a] for the investigation of the climate sensitivity of the subice circulation beneath Filchner Ice Shelf. Bedrock topography and ice shelf draft is taken from the digital IfAG-map [*Vaughan et al*., 1994] and calculated from ERS-1 satellite data [*Wingham et al*., 1997], respectively.

The Filchner Trough is ~600 km long with increasing depth to the south, separating the Berkner Bank with water depth <300 m to the west from the Coats Land shelf to the east. About half of the trough is located beneath the Filchner Ice Shelf. According to *Melles et al*. [1994], the zonal profile of the trough is asymmetric with a more gentle western slope (0.3°) and a steeper eastern flank (1.1°). The bottom depth increases from 600 m at the sill in the north to 1200 m at the ice shelf front and reaches >1400 m beneath the central ice shelf. The deepest northern part of the sill, with a depth of ~600 m, is only ~50 km wide. North of the sill and shelf break is the steep continental slope to the deep sea.

In order to provide a link to the deep Weddell Sea an open northern boundary was set along the continental shelf break, applying a numerical boundary condition after *Stevens* [1991] (marked area in Figure 2). Following *Foldvik et al*. [1985a, 1985b], who found a barotropic flow of 0.7–1.0 Sv (1 Sv = 10^6 m^3 s^{-1}) directly north of the Filchner Trough, we specified a barotropic outflow at the sill of 1 Sv along the western flank of the deepest outlet of the depression (35°–30°W) and an equivalent inflow in the east. In areas where the current is mainly parallel to and westward along the shelf break, no barotropic flow ($\Psi = 0$) perpendicular to the boundary along the shelf break was prescribed. The model computes cross-boundary velocities that take into account wave propagation out of the domain, allowing water to leave the cavity without having any effect on inflowing water. This is consistent with our measurements indicating a clear separation between the inflow and outflow (see Figure 5, stations 148–192). Outflowing waters

are carried by the coastal current to the west, while inflowing waters come from the east. At inflow points, heat and salt is advected into the model domain, restoring temperature and salinity along the boundary to a measured profile of 1995 (see Figure 5a and 5b) using a Newtonian damping of 100 days.

The model is forced by a 3-year mean European Centre for Medium-Range Weather Forecasts (ECMWF) wind field [*Kottmeier and Sellmann*, 1996], a simple thermodynamic sea ice model for the open ocean, and buoyancy fluxes due to melting and freezing in the subice shelf cavity. The time-averaged wind field lacks seasonal atmospheric forcing and, consequently, realistic sea ice formation and salt rejection, which makes a dynamic component for the sea ice unnecessary. The sea ice model is an analog to that described by *Grosfeld et al*. [1997], utilizing a simple thermodynamic coupling with the atmosphere to calculate surface salt fluxes. The surface freezing point of seawater is fixed at −1.9°C, and heat fluxes across the surface are calculated from temperature differences to the uppermost ocean layer, permitting equivalent melting and freezing rates and related salt fluxes to the ocean to be calculated. Although this is a diagnostic approach for areas where waters colder than the surface freezing point reach the ocean surface and the model also excludes advection of sea ice, we included the effect of a seasonal ice variation on the water mass characteristics. In ice-free regions an additional restoring is applied by prescribed surface salinities and temperatures, varying sinusoidally from 34.4 in summer to 34.6 in winter. As the shallow Berkner Bank is known to be one of the major areas for High-Salinity Shelf Water production [*Foldvik et al*., 1985a], salinities in that area south of 76°30′S are adjusted to the 1995 measurements (see section 3, Figure 6). Variations in the strength of the restoring conditions on Berkner Bank are neglected because our central aim is to investigate the influence of the displacement and grounding of icebergs and related changes in the circulation pattern and water mass formation. Changing the boundary conditions would also make it difficult to distinguish between the impacts of the icebergs and different restoring conditions.

A similar procedure is applied to the area south of Berkner Island in the Thiel Trough to prevent desalination due to melting processes in the deep cavity. There we restore to temperature and salinity profiles taken from a simulation for the whole Filchner-Ronne Ice Shelf [*Gerdes et al*., 1999]. That model showed that only weak trough flow exists south of Berkner Island. As *Nøst and Østerhus* [1998] have noted, the grounding of the icebergs yields an increased flow of dense waters from the Ronne Ice Shelf to the Filchner Trough south of Berkner Island. As the model has an artificial closed boundary there, a variation in the through flow in the Thiel Trough cannot be considered. A possible effect in the model can therefore only be expected through changes in the current transport in the southernmost Filchner cavity due to changes in the northern inflow.

The model results are snapshots after integration of 10 years from an ocean at rest, when a quasi-steady state is reached. Initialization occurred with constant salinity (34.60) on all levels and vertical homogeneous temperature of −1.9°C in the open ocean, decreasing by 0.1°C per degree of latitude beneath the ice shelf. After the initial model run representative for the scenario before 1986, integration continues for 4 years with a new ice shelf front position and three icebergs grounded on the eastern Berkner Bank. To simulate the 1990 departure of iceberg A24 from the Filchner Trough, the integration is carried out for another 5 years with the two remaining western icebergs ending at the time of the measurements in 1995, 9 years after the calving event.

3. Observational Program and Hydrographic Sections in 1995

In February 1995, CTD profiles were measured from RV *Polarstern* during cruise ANT XII/3 with a Falmouth Scientific Instruments Triton CTD and corrected by a salinometer Autosal 8400. The accuracy of the CTD data is better than 0.003 in salinity, 3 mK in temperature, and 3 dbar in pressure. More detailed information about the calibration process is given by *Schröder and Fahrbach* [1999]. For oxygen isotope determinations, 7 mL of water were equilibrated in 13 mL head space with CO_2 gas by using an automated Finnigan HDO device. Isotope equilibrium in the CO_2-H_2O system was attained by shaking for 430 min at 20°C. The equilibrated gas was purified and transferred to an on-line connected Finnigan MAT Delta-S mass spectrometer. Isotope measurements were calibrated against Vienna standard mean ocean water (VSMOW) and Vienna standard light Antarctic precipitation (VSLAP) standard waters. The external reproducibility was ±0.03‰ at 1σ. At least two replicates (including preparation and measurement) were run for each oxygen isotope determination.

The data set used here consists of three sections (Figure 3). We next describe the hydrographic conditions revealed by these sections, using the following water mass terms (see also Table 1): Warm Deep Water (WDW) with temperatures between 0° and 0.8°C and salinities between 34.64 and 34.72 [*Foldvik et al*., 1985a] is advected by the Weddell Gyre into the southern Weddell Sea as source water of circumpolar origin. This water is transformed near the shelf break to Modified Warm Deep Water (MWDW) ($34.45 < S < 34.64$, $-1.2°C < \Theta < 0.2°C$) by mixing with Antarctic Surface Water (ASW) ($S < 34.30$, $-1.7°C < \Theta$), which represents the surface layer of the open Weddell Sea in summer, or Winter Water (WW) ($34.30 < S < 34.45$, $\Theta < -1.7°C$) in winter. On the shelf, water properties are determined by different processes. Eastern Shelf Water (ESW) ($S < 34.45$, $-1.9°C < \Theta < -1.7°C$) has a low salinity from glacial meltwater [*Fahrbach et al*., 1994] and sometimes cannot be distinguished from WW advected onto the shelf. Hence we combine these two water masses under the Low-Salinity Shelf Water (LSSW) label ($34.30 < S < 34.45$, $-1.9°C < \Theta < -1.7°C$). High-Salinity Shelf Water (HSSW) ($34.65 < S$, surface freezing point $< \Theta < -1.7°C$) is formed by the enrichment in salinity during freezing of sea ice on the southern continental shelf. All water with potential temperature below the surface freezing point is called Ice Shelf Water (ISW).

3.1. Section 1

The Filchner Trough below 550 m depth is filled with ISW of $\Theta < -2.0°C$ and salinities of 34.58 to −34.65 (Figures 4a and 4b). Two ISW cores emanate from the Filchner cavity at the western flank of the trough, one near 700 m depth and a shallower one near 150 m depth. Both have densities of $\sigma_\Theta \approx$ 27.880 and are most likely connected, but owing to the large distance between stations 184 and 196 a separation cannot be excluded. In the deep core at station 197 the potential temperature attained a minimum of $\Theta = -2.246°C$ with a salinity of 34.621 at 826 m depth, whereas the shallower core at 155 m

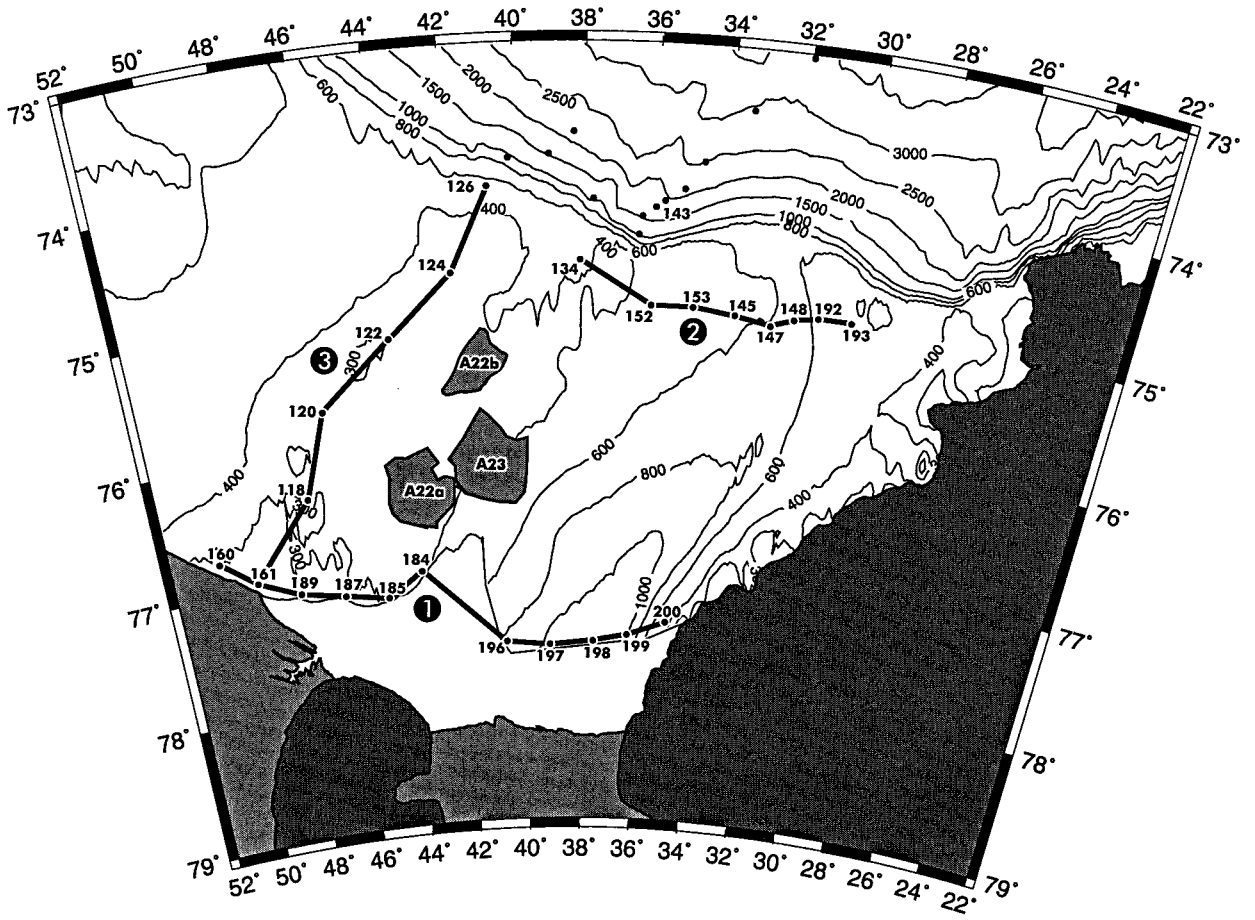

Figure 3. Stations taken on RV *Polarstern*, leg ANT XII/3 1995. CTD stations discussed in this study are indicated with numbers. The positions of icebergs in 1995 and the fast ice edge are marked. Ice shelf and inland ice area are shaded. Sections shown in Figures 4, 5, and 6 are indicated by thick lines.

depth at station 184 is significantly warmer with $\Theta = -2.064$°C, but only slightly more saline at s = 34.623.

A δ^{18}O minimum (less than -0.55‰) at station 199 at 200 m depth shows that parts of the shallower core of ISW recirculate on the east side of the depression shortly after leaving the ice shelf (Figure 4c). Because of higher δ^{18}O values at the northern inflow of the trough (see Figure 5c) this minimum has no other possible source. After *Weiss et al.* [1979], δ^{18}O concentrations of less than -0.50‰ indicate the admixture of glacial meltwater to seawater. Dominant outflow along the western flank of the trough is indicated by δ^{18}O contents of up to -0.79‰. Higher δ^{18}O values in the eastern part of the deep trough show increased portions of MWDW and/or HSSW, originating from entrainment in the northend of the Filchner Trough advected with the main circulation to the south. However, the signal clearly indicates recirculating ISW, as first suggested by *Carmack and Foster* [1975].

Table 1. Definition of Water Masses Near Their "Source" Regions[a]

Water Mass	Θ, °C	*S*
ASW	greater than −1.7	<34.30
WW	less than −1.7	34.30–34.45
ESW	−1.9 to −1.7	<34.45
LSSW	−1.9 to −1.7	34.30–34.45
MWDW	−1.2–0.2	34.45–34.64
WDW	0–0.8	34.64–34.72
ISW	less than −1.9	
HSSW	−1.9 to −1.7	>34.65

[a]ASW, Antarctic Surface Water; WW, Winter Water; ESW, Eastern Shelf Water; LSSW, Low-Salinity Shelf Water; MWDW, Modified Warm Deep Water; WDW, Warm Deep Water; ISW, Ice Shelf Water; HSSW, High-Salinity Shelf Water. Θ is potential temperature; *S* is salinity in practical salinity units.

On Berkner Bank (stations 160–184) the 50–100 m thick bottom layer with salinities of $S > 34.650$ and densities of $\sigma_\Theta > 27.90$ consists of HSSW. This water is also found in the bottom layer on the eastern side of the trough at stations 198 and 199 but mixed with recirculating ISW, as revealed by temperatures below the surface freezing point and δ^{18}O values from -0.60 to -0.65‰.

3.2. Section 2

The salient feature of section 2, located ~15–40 km south of the sill between the Filchner Trough and the continental slope to the Weddell Abyssal Plain, is an outflowing core of ISW below 250 m at stations 153, 145, 147, and 148 that is flanked by MWDW inflow on both sides (Figures 5a and 5b). Above these we find ESW in the eastern part of the section (stations

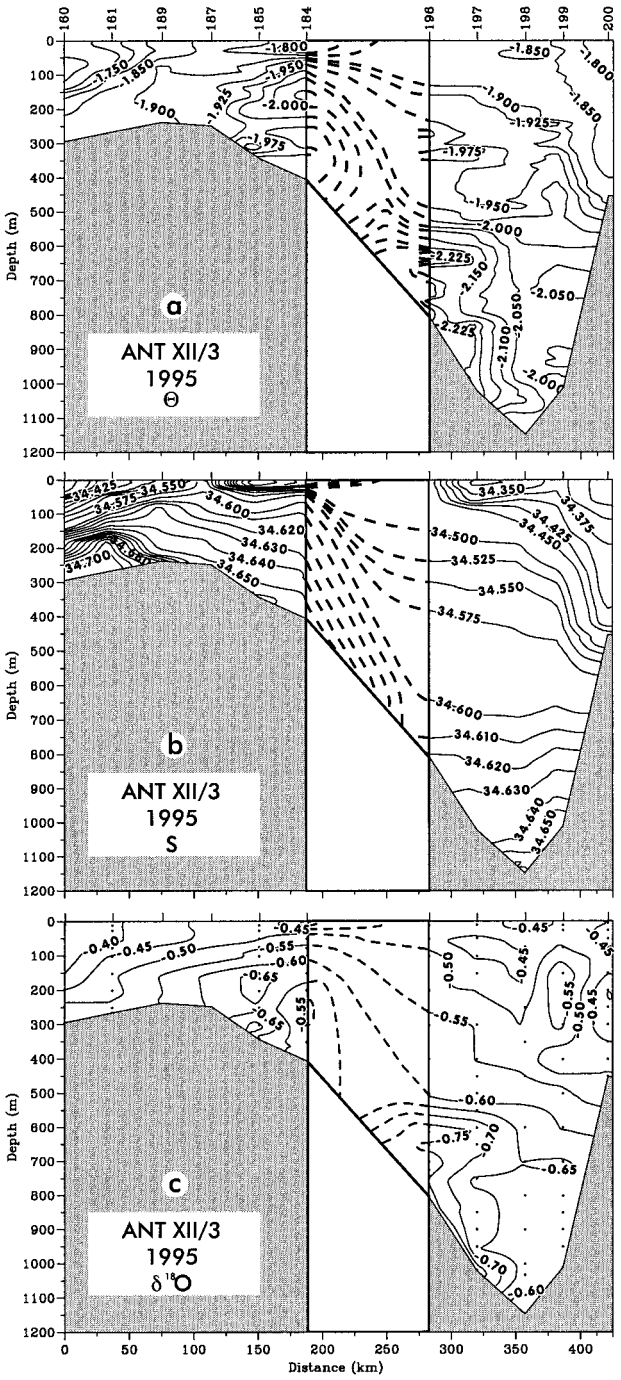

Figure 4. (a) Potential temperature (in °C), (b) salinity (in practical salinity units), and (c) $\delta^{18}O$ (in ‰) distribution of section 1 (Figure 3) along the fast ice edge in front of Filchner Ice Shelf. Because of the large distance between stations 184 and 196 the distribution of the tracers cannot be given with the same accuracy as the remaining parts and therefore are indicated with dashed contours.

148–193). In the central part of the passage the ESW layer merges into a WW layer, both together being part of the LSSW. Under the ISW and MWDW a thin bottom layer consists of HSSW with a temperature near $\Theta = -1.90$°C and a salinity of $S > 34.65$. The density in this layer exceeds 27.92, which is by far the most dense water in this area. It originates on the southern Berkner Bank in front of the eastern Ronne Ice Shelf nearly 280 km farther south. A mixture of HSSW and ISW is present near the sill at a density of 27.88–27.92, one of the potential components of Weddell Sea Bottom Water.

The distribution of $\delta^{18}O$ (Figure 5c) reveals the lowest values (<-0.50‰) in the ISW core in the center of the outlet. Bottom values are slightly higher in the HSSW layer compared to its source area on Berkner Bank. This reflects mixing between HSSW and adjacent ISW on its way north, as discussed later in section 5. The MWDW core at station 134 at 360 m depth and at station 192 at ~450 m depth is marked by a local maxima in $\delta^{18}O$ derived from the WDW, which is characterized by an overall maximum of −0.07‰ [*Schlosser et al*., 1990]. The scheme of the regional distribution of the water masses on the northern sill of the Filchner Trough compiled in Figure 5d summarizes the observational results for this region.

3.3. Section 3

This meridional section (stations 161–126) starts at the fast ice edge north of Berkner Island and ends at the continental slope to the Weddell Abyssal Plain at 500 m depth. For this study we focus on the southern part located on the shallow Berkner Bank because it characterizes the western boundary of the model domain. The core of the HSSW plume with salinities >34.680 and temperatures of less than −1.80°C is formed in the polynya in front of Berkner Island and can be traced northward only up to station 118 (Figures 6a and 6b). Farther north up to station 124, only the 50 m nearest the bottom are partly influenced by the HSSW plume but with a more westward flow direction, deduced from the vessel-mounted acoustic Doppler current profiler. Therefore this water is not involved in the overflow process at the Filchner sill (Section 2). North of station 120 the water column is strongly influenced by a tongue of MWDW which spills onto the shelf from the north and extends southwestward toward the Ronne Ice Shelf front farther to the west. Hence the characteristics of water near bottom on the outer shelf are modified to higher temperatures (up to −1.3°C) and lower salinities (of <34.610), while MWDW is freshened above by LSSW. The location and extension of the HSSW plume on this section, at stations farther east (189 and 187, Figure 4b), and in section 2 (Figure 5) suggests that it follows depth contours to the northeast. This is confirmed by the $\delta^{18}O$ distribution (Figure 6c). Typical values in the HSSW plume within 100 m of the bottom at stations 161 and 118 range between −0.40 and −0.50‰ versus <−0.45‰ on the sill as shown in Figure 5c. These slightly decreased $\delta^{18}O$ values along the flow suggest mixing with the adjacent ISW outflow from the ice shelf cavity.

4. Model Simulations for Different Stages of the Calving Event

In the following, three different model simulations for the iceberg calving event at the Filchner Ice Shelf front are discussed. They represent scenarios during three different morphological settings caused by the formation and displacement of the icebergs: (1) the precalving scenario representative of a quasi-steady state condition before 1986, (2) the period between 1987 and 1990, when three icebergs were partly grounded on Berkner Bank, and (3) the scenario between 1990 and 1995, where one iceberg had left the trough and the remaining ones moved. The latter condition exists when the 1995 hydrographic measurements were taken in the Filchner Trough.

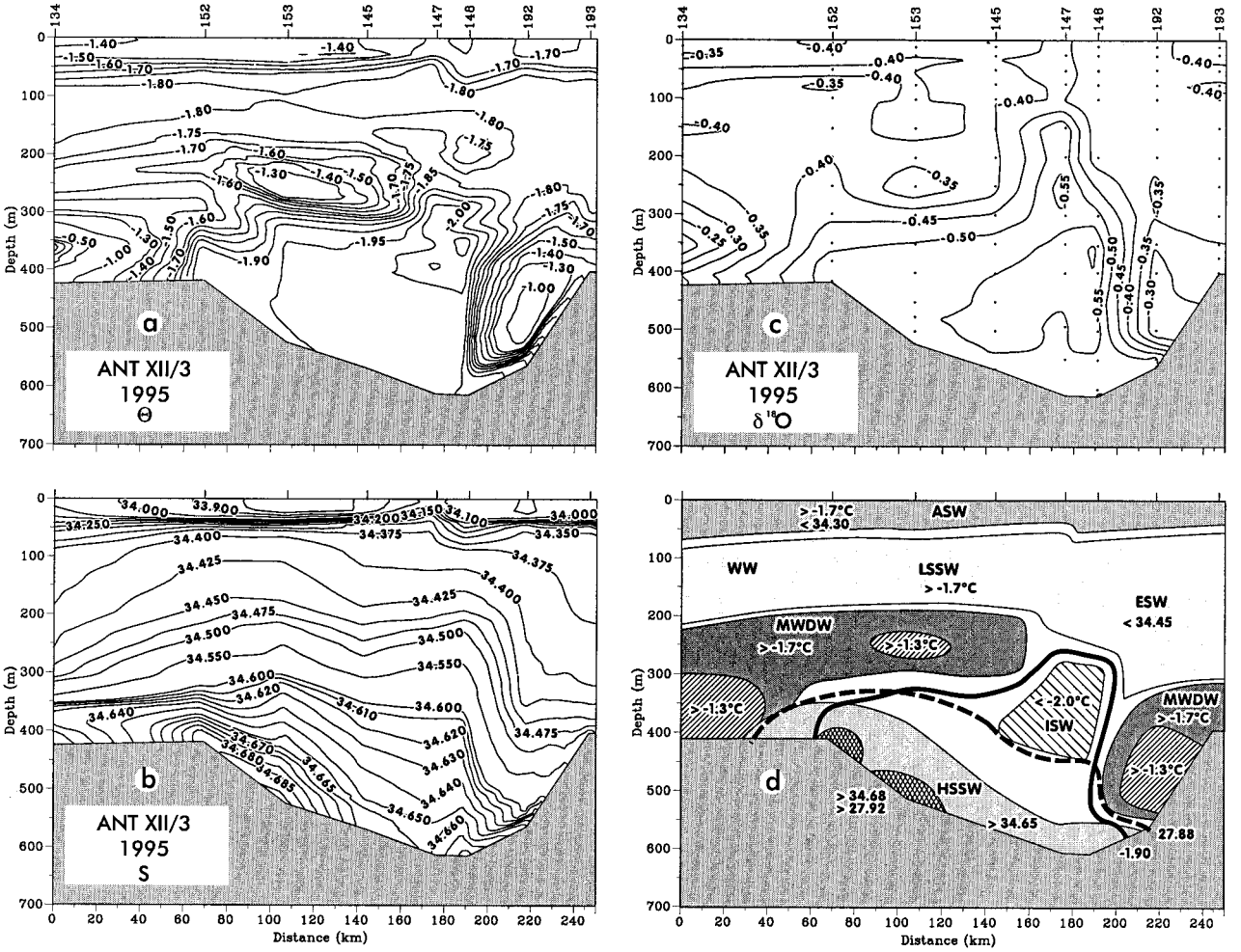

Figure 5. (a) Potential temperature, (b) salinity, (c) $\delta^{18}O$, and (d) a schematic water mass distribution of section 2 (Figure 3) along the Filchner sill. Strong horizontal gradients separating inflow and outflow occur east of station 148. The thick solid line is drawn around water with temperatures less than −1.9°C, and the thick dashed line is drawn where densities exceed 27.88. This density range is favorable for bottom water formation.

4.1. Precalving Scenario

The vertically integrated mass transport streamfunction for the precalving scenario (Figure 7) shows a cyclonic gyre in the depression north of the ice shelf. The southward flow from the sill of ~1.8 Sv along the eastern flank of Filchner Trough transports MWDW from the shelf break. This water mass is prescribed to enter the model domain across the open boundary at a rate of 1 Sv over the eastern flank of the deepest outlet along the sill (see Figure 5). The main gyre is located in the interior of the trough and increases to ~2.3 Sv, causing enhanced recirculation rather than meridional exchange south of 76°S. A northward flow of ~1 Sv occupies the northern part of the Berkner Bank. The northern boundary of the model domain, which is positioned along the continental shelf break, forces eastward transport over the Berkner Bank, opposing the coastal current at the continental shelf break. Model experiments with a larger domain, including the open ocean beyond the shelf break, show an analogous pattern of a gyre in the Filchner Trough with a small outflow across the sill at ~32°W. In addition, a model simulation covering the whole Filchner-Ronne Ice Shelf domain, including the continental shelf seaward of the ice shelf [*Grosfeld and Gerdes*, 1998b], shows a similar strong cyclonic circulation cell in the center of the trough and a northeastward flow on the northern Berkner Bank. This sets west, when the topography falls to the deep sea. *Beckmann et al*. [1999] detected a strong westward shelf break current and a cyclonic cell in the Filchner Trough in the annual mean, vertically integrated transport function, using a coarse-resolution model for the Weddell Sea. All of these results indicate that the artificial boundary of this regional model set up is of minor importance for the general flow pattern in the domain which depicts a plausible circulation system.

In front of the ice shelf at 77.9°S the vertically integrated flow abruptly turns westward due to the reduction in water column depth by the ice shelf front, which steers barotropic flow along the ice shelf front [*Grosfeld et al*., 1997]. Only 0.4–0.6 Sv enter the cavity west of the steepest bottom slope, with the main gyre reaching ~80.5°S. The eastern and southernmost parts of the cavity are only barely influenced by the main circulation because of the small water column thickness of 100–300 m in the east compared to ~600–800 m in the main trough. Circulation in the Thiel Trough is weak because the thermohaline forcing by melting or freezing at the ice shelf base is weak.

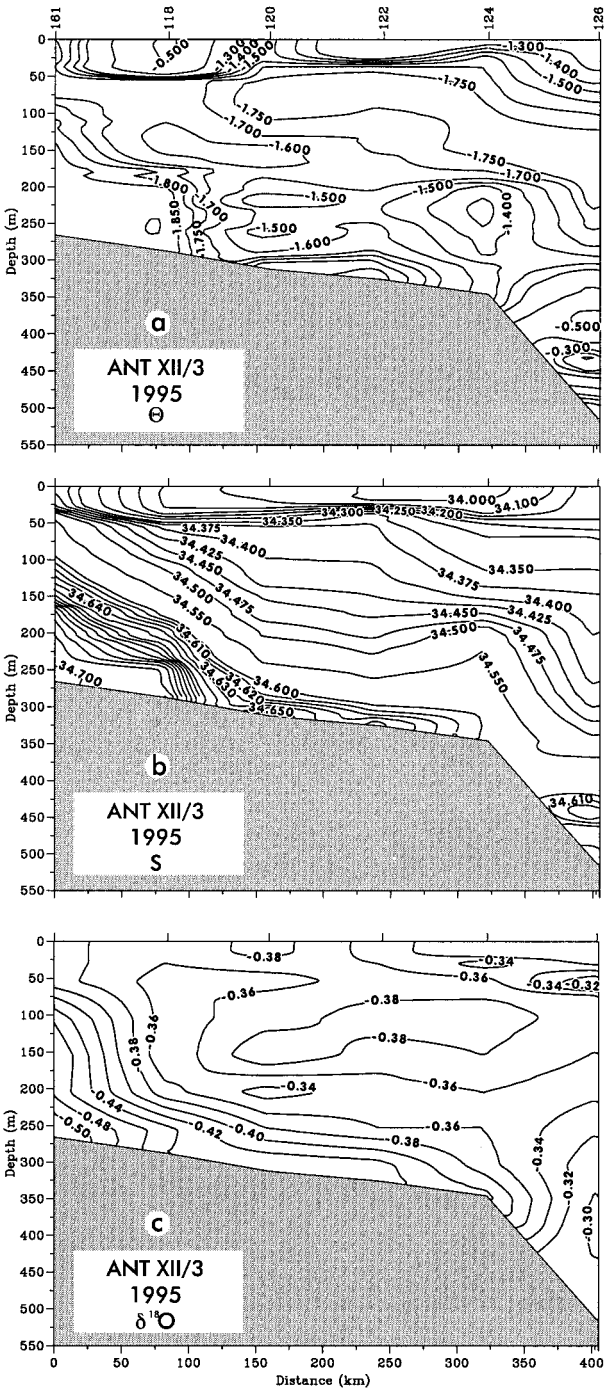

Figure 6. (a) Potential temperature, (b) salinity, and (c) $\delta^{18}O$ of section 3 (Figure 3) from south to north across the Berkner Bank. Stations 161 and 118 depict the area where HSSW production occurs on Berkner Bank.

Although recirculation in the deep cavity is also influenced by the artificial closed boundary over the Thiel Trough, a comparison with model results from *Gerdes et al*. [1999] shows that only weak net through flow exists south of Berkner Island. Interactions between the Ronne and Filchner Ice Shelf cavities occurs mostly by gyre-to-gyre interaction rather than by direct flow. This is confirmed by the 1980 measurements of *Nøst and Østerhus* [1998] (see Figure 10a, dashed line '80w), which indicate no distinct Ronne Trough component but a mixture with waters from Berkner Bank during the precalving state. A more advective component of the flow leading to a clearer Ronne Trough signal in this model configuration depends on the prescribed boundary condition in the Thiel Trough and is not implicitly included. Nevertheless, the artificial closing of the domain south of Berkner Island seems not to give an incorrect flow regime, except that the Θ/S characteristics depend on the prescribed values, and fluctuations imposed by an intensified Ronne Ice Shelf inflow are not represented.

From the cavity volume and a mean transport of 0.4–0.6 Sv in the central trough we estimated residence times of 1.4–2.0 years for waters in the central part of Filchner Ice Shelf cavity. Because the southern and especially the eastern parts of the cavity are not reached by the main circulation, the residence times for water masses in those areas are more than twice that in other areas.

Spreading of HSSW in the bottom layer (Figure 7b) demonstrates the ventilation mechanisms for the Filchner domain in the model. Southern Berkner Bank, where salinities were restored to 34.58–34.7 (from top to bottom), is influenced by outflowing waters from the ice shelf cavity. Because the water column beneath the ice shelf along the eastern grounding line of Berkner Island is very shallow (<100 m), the outflows are enriched in meltwater from the ice shelf base as indicated by the local salinity minimum of 34.52 south of the western part of the ice front. The salinity of the waters more to the west on Berkner Bank range between 34.68 and 34.6. North of ~77.5°S, the influence from the restoring becomes obvious, as waters spread from the west into the deep trough. In addition, waters with salinities of 34.6–34.62 enter the trough from the north through the prescribed inflow along the depression at the sill. Compared to measurements in the Filchner Trough, the modeled bottom salinity in the eastern part of the trough is ~0.05 too low.

A temperature cross section along the ice front Figure 7c indicates a cold ISW plume emanating from the ice shelf cavity at the western side along Berkner Island with two cores. A shallow core originates at the ice shelf base, and a deep core at ~700 m depth indicates a detachment of ISW from the base within the ice shelf cavity. The eastern part of the cross section depicts waters which are obviously influenced by the admixture of surface waters or MWDW from the north. The general hydrographic structure compares well with earlier observations, although the temperature range is partly too warm.

The model shows ISW reaching the surface in the open ocean and therefore where sea ice formation may be induced by the upwelling of supercooled waters. *Dieckmann et al*. [1986] sampled a large volume of ice platelets along the western part of the Filchner Ice Shelf front in the outflow regime from the subice shelf cavity and noted indications that these ice platelets rise to the surface and contribute to sea ice formation. The model simulation depicts a narrow zone of fast ice, formed by freezing at a rate of >3 m yr^{-1} through upwelling of ISW at the northeastern edge of Berkner Island (Figure 7d). This is about twice the rate of basal freezing beneath the northwestern part of the ice shelf. For a detailed discussion of the basal mass balance beneath the ice shelf, see *Grosfeld et al*. [1998]. However, most ISW is advected northwest and mixes with ambient waters, so that no significant area of sea ice formation occurs by upwelling of ISW.

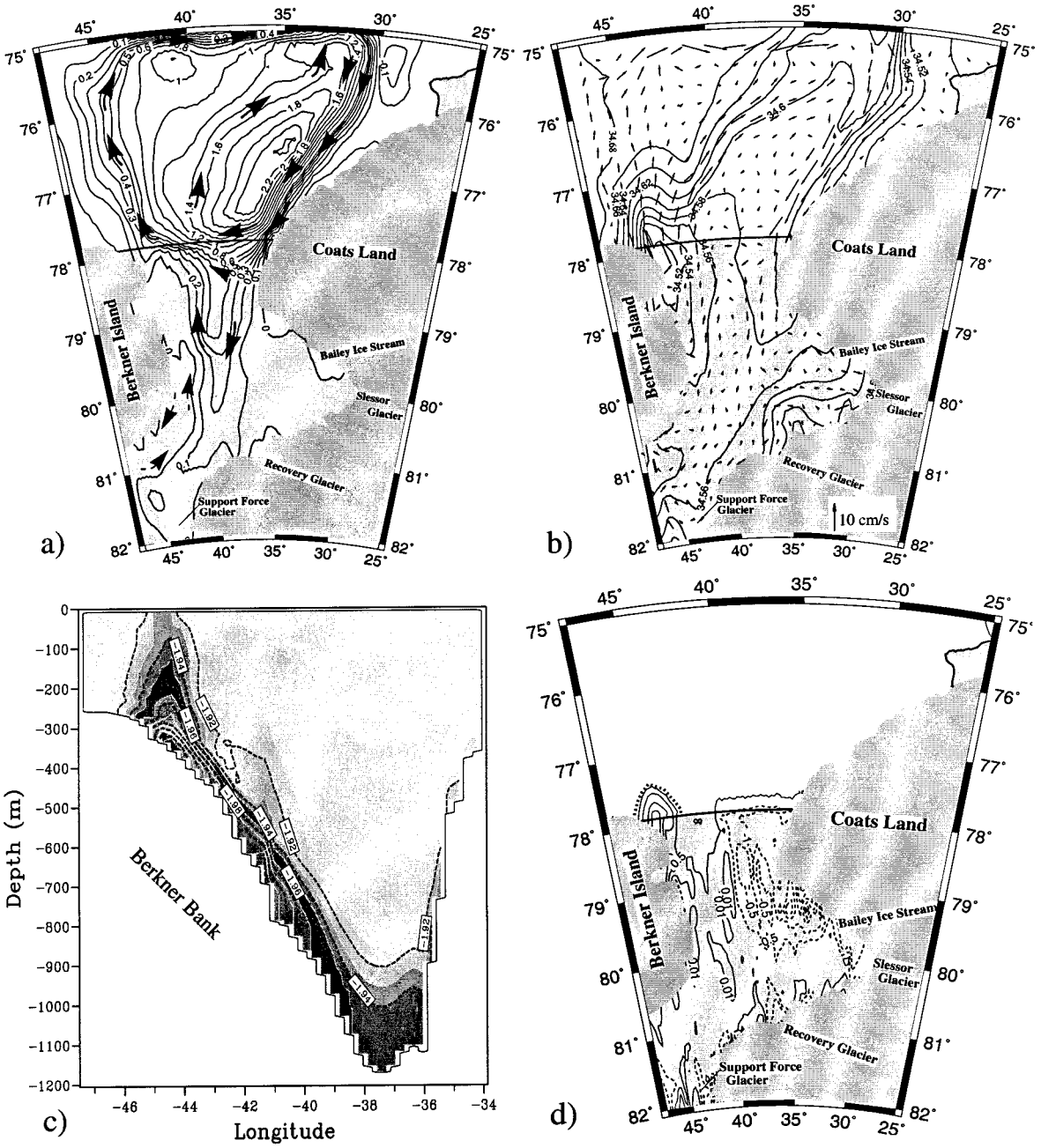

Figure 7. (a) Stream function for the vertically integrated mass transport (in Sv) and (b) bottom salinity distribution and bottom velocities (in cm s^{-1}) for the precalving scenario derived from modelling results. Contour interval in Figure 7a is 0.1 Sv below 0.5 Sv and 0.2 Sv above. Between 30° and 35°W a barotropic inflow and outflow of 1.0 Sv is prescribed. (c) Temperature cross section along the ice shelf front (in °C) indicating ISW outflow at the western slope of the trough. (d) Fast ice extent (dotted line) as derived from the model results and freezing rate (in m yr^{-1}; dashed lines indicate melting) of marine ice beneath and in front of the Filchner Ice Shelf.

4.2. Postcalving Scenario Between 1987 and 1990

After calving in August 1986, icebergs A22, A23, and A24 drifted for ~1 year to the northwest with the cyclonic circulation in the Filchner Trough. Because of their draft the two westerly icebergs, A22 and A23, grounded on the Berkner Bank at the 400 m depth contour, while A24 first assumed the former position of A23 for about half a year and then remained afloat east of the grounded A23 in the trough (Figure 2). Simulation of the ocean circulation during the first 4 years after the calving event was carried out with three islands placed at the mean iceberg positions over this period and with the ice shelf front at 78.3°S.

Compared to the precalving scenario, the center of the main gyre in the Filchner Trough is shifted southward and decreased in its extent and transport (Figure 8a). The southern part of the gyre is separated from the north, where short recirculation loops and an anticyclonic countergyre arise instead of the large-scale extension of the main gyre. The main circulation is

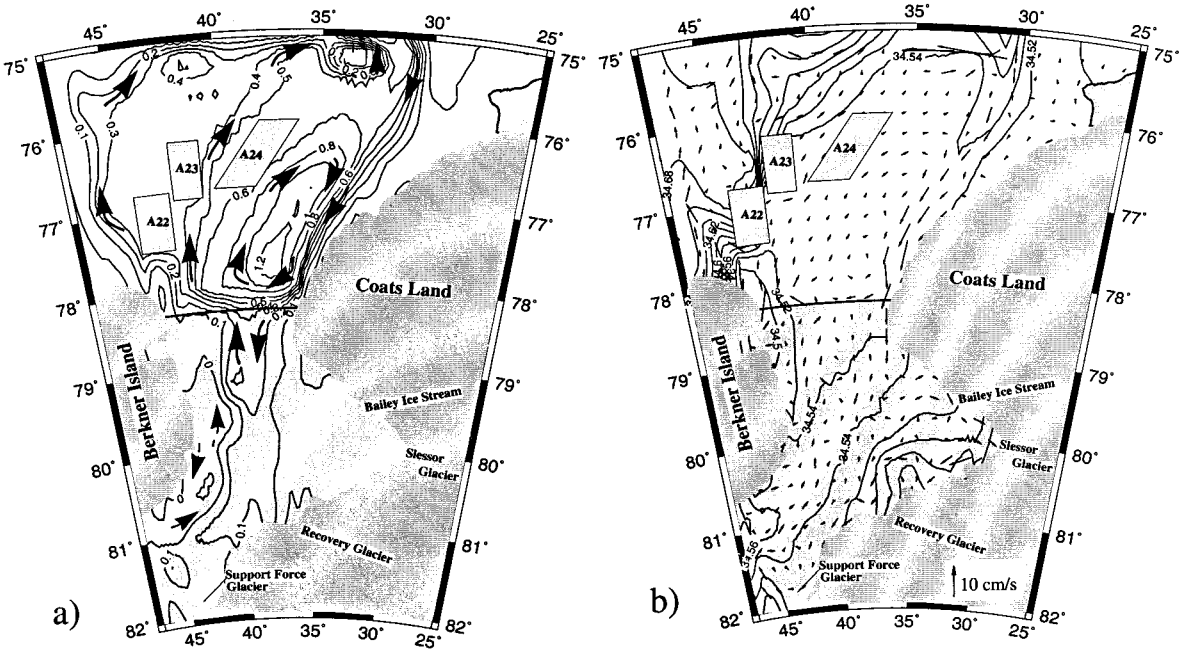

Figure 8. (a) Stream function for the vertically integrated mass transport (in Sv) for the postcalving scenario between 1987 and 1990, when all three icebergs are grounded along the Berkner Bank and the ice shelf front has retreated ~0.4° in latitude. Contour interval is 0.1 Sv below 0.5 Sv and 0.2 Sv above. (b) Bottom salinity distribution and bottom velocities (in cm s^{-1}) for the same scenario.

located southeast of the icebergs with a maximum transport of 1.2 Sv. The circulation in the ice shelf cavity is strongly reduced to 0.2 Sv at its maximum and occupies only the northern part of the cavity up to 79.5°S. In the deep cavity a background circulation of 0.1 Sv remains because of the east-west density differences. Because of the northward retreat of the central gyre in the cavity the anticyclonic gyre along Berkner Island increases in extent and strength and moves more to the north. With an open western boundary in the Thiel Trough this increased flow could lead to an enhanced flow of saline waters from the Ronne Ice Shelf cavity, eventually originating on Berkner Bank and flowing west of Berkner Island to the south or taking a long path from the Ronne Trough. With the recent model configuration an increase in bottom salinities is not detected since the water characteristics in the restoring zone have not been altered. Waters from the deep cavity and south of Berkner Island are able to protrude farther to the north, however, by the retreat of the northern circulation cell.

Water exchanges between Berkner Bank and the Filchner Trough are largely blocked by the icebergs. HSSW flow is deflected from the deep trough and takes a more northerly course toward the shelf break (Figure 8). The source region for HSSW is now located west of the icebergs, on the western slope of Berkner Bank, out of range of the Filchner Trough circulation. This leads to a decrease of ~0.06 in the bottom salinity of the deep trough.

On the southern Berkner Bank the salinity of HSSW does not increase in spite of the smaller export rate because the formation area is reduced by the grounded icebergs, decreasing sea ice production and brine rejection. Outflowing ISW from the ice shelf cavity is steered along the east side of the icebergs, sea ice drift is blocked, and a fast ice tongue develops on their east side. This result is consistent with a satellite image analysis [*Markus*, 1996] that showed the polynya moving from a position in front of the Filchner Ice Shelf and Berkner Island to a north-south orientation at the western (lee) side of the icebergs. The National Ice Center charts (see http://www.natice.noaa.gov) depict a 10/10 ice cover east of the icebergs over the whole year, confirming the existence of a fast ice tongue in this area.

The grounded icebergs may allow more dense waters to drain westward into the Ronne Trough and underneath the Ronne Ice Shelf. Another consequence of the grounding is that some HSSW takes a longer route around the icebergs (compare Figures 8b and 7b). This may lead to a change in the direct overflow of HSSW at the continental shelf break influencing deep and bottom water formation in the Weddell Sea.

4.3. Postcalving Scenario Between 1991 and 1995

After iceberg A24 had left the Filchner Trough, A22 and A23 slowly moved north. In early 1994, A22 broke in two parts, one of which moved north of A23. The mean positions of these icebergs are therefore represented in the third model configuration as two islands shifted ~50 km to the north. This is the location of the icebergs during the measurements carried out in 1995 (Figure 3).

Contrary to the previous scenario, northward recirculation of the main gyre in the Filchner Trough now takes place over its western slope (Figure 9a). Nevertheless, the counterrotating gyre at the northern boundary still exits, implying that the system has not fully switched back to the precalving state. The transport in the trough of 0.95 Sv is less than the two earlier model runs but extends over the whole trough, comparable to the precalving scenario. Flow into the ice shelf cavity increases in this model run to 0.35 Sv and reaches farther to the south (up to 80°S), increasing ventilation of the ice shelf cavity.

Repression of the anticyclonic cell along Berkner Island indicates a reduced influence of waters from the deep cavity

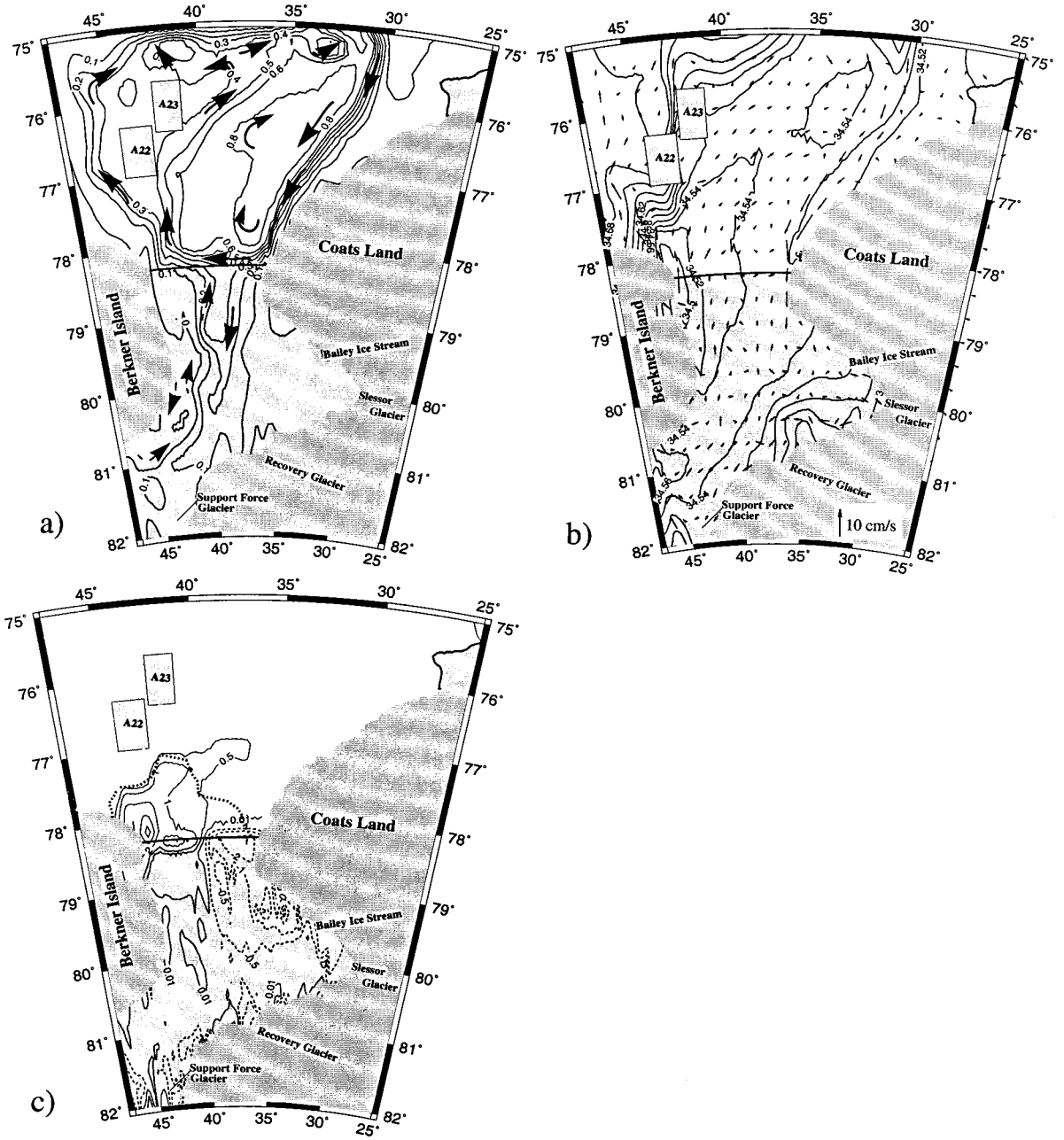

Figure 9. (a) Stream function for the vertically integrated mass transport (in Sv) for the postcalving scenario in 1995, when iceberg A24 has left the trough and the hydrographic measurements were obtained. Contour interval is 0.1 Sv below 0.5 Sv and 0.2 Sv above. (b) Bottom salinity distribution and bottom velocities (in cm s^{-1}) for the same scenario. The northward shift of the icebergs leads to a slow increase of HSSW flow into the trough. (c) Fast ice extent (dotted line) as derived from the model results and freezing rate (in m yr^{-1}; dashed lines indicate melting) of marine ice beneath and in front of the Filchner Ice Shelf.

south of Berkner Island on the characteristics of the outflowing water at the ice shelf edge. The circulation over Berkner Bank is still weak, as both icebergs occupy most of the area. The bottom salinity distribution (Figure 9b) shows HSSW spreading into the trough along the southeastern edge of the icebergs, but they still deflect most of the densest water into a northwestward path. Waters in the deeper part of the trough are thus ~0.06 less saline, compared to the scenario before the 1986 calving event. This result is in good agreement with *Nøst and Østerhus* [1998], who found freshening of 0.1 in their 1993 measurements compared to 1984.

The reduction of HSSW in the deeper part of the trough also has consequences for the temperature distribution [*Grosfeld and Gerdes*, 1998a]. Less dense water in the Filchner Trough leads to a reduction of the flow of waters with temperatures close to the surface freezing point into the deep ice shelf cavity (Figures 8 and 9). This again reduces the total heat content in the cavity and changes the ice shelf–ocean mass exchange, and

colder waters then exit the cavity. Bottom temperatures in the Filchner Trough in front of the ice shelf are up to 0.1°C colder than in the precalving scenario.

Upwelling of ISW and blocking of the flow to the west lead to the formation of a larger fast ice tongue than in the precalving scenario (Figure 9c). The model results depict a permanently ice-covered area, which compares well with observations in 1995 (Figures 1). With a freezing rate of 4 m yr^{-1} an ice tongue of 40 m thickness or more could have been built since 1986. This tongue could provide an opportunity to study the formation process of marine ice, an ice class which normally is only accessible beneath hundreds of meters of meteoric ice under the large ice shelves.

5. Discussion of Water Mass Characteristics

The grounding of three huge icebergs on the Berkner Bank changed the water mass distribution in this region. Model experiments showed that calving, displacement, and grounding of the icebergs shifted the source region for HSSW production more to the west, out of the range of the central gyre within the Filchner Trough. Consequently, a reduction occured in the flow of dense waters from Berkner Bank into the trough and ice shelf cavity. With the reduced thermohaline forcing, less saline waters then occupy the bottom layers in the trough, the vertically integrated mass transport slows, and the circulation in the ice shelf cavity becomes less active.

Water in the cavity cools because less water with HSSW properties enters from the north, while colder water from the south spreads farther northward. The latter effect is due to the weaker Filchner gyre. From these results the flow in the Filchner Trough can be described as a circulation driven by two different sources, i.e., from Berkner Bank and from south of Berkner Island. Although the model results cannot show the increased influence of Ronne Ice Shelf waters on the south source, owing to the closed boundary there the blocking effect of the icebergs on the hydrography and circulation in the Filchner Trough is clear. After 1990, when the first iceberg drifted away, the inflow of water from Berkner Bank increased, and the system began to switch back to the precalving state.

With the above background we can evaluate hydrographic measurements taken near the Filchner Ice Shelf over time in this dynamically evolving system. Measurements from 1980 and 1989 from *Nøst and Østerhus* [1998] are shown together with our 1995 in Figure 10. The precalving condition 1980 on the western flank of the Filchner Trough is depicted by station 163, and the water mass distribution over the central and eastern trough is depicted by station 5 (Figure 10a). Conditions in the Filchner Trough shortly after the calving event are depicted by station 26 on the western slope and station 24 in the central part in 1989 (Figure 10b).

Water mass properties ~9 years after the retreat of the ice shelf front are represented by the 1995 data at approximately the same locations as the historical profiles. Station 196 on the western slope and station 198 in the central part (compare with Figure 4) are shown as thick lines in Figure 10a. In addition, the surface freezing line (thin dashed) and two theoretical mixing lines (solid lines, M_B and M_R) are displayed. According to *Gade* [1979] and *Nøst and Foldvik* [1994], these mixing lines represent the temperature-salinity correlations for ISW formed from different types of HSSW and the input of freshwater due to melting at the ice shelf base. The heat loss by the seawater due to melting is proportional to the meltwater gain (freshening) of the residual water mass. Heat conduction within the ice shelf is neglected because the effect is comparably small [*Nøst and Østerhus*, 1998]. The HSSW types have temperature at surface freezing point but with salinity values representing the conditions of waters in the polynya in front of the ice shelf at different geographical positions. For M_B a salinity of 34.70 is used, near the maximum observed on Berkner Bank. The M_R salinity 34.75 denotes water parcels from the Ronne Trough because that salty (dense) water is only found west of 55°W.

The shaded areas in Figure 10 depict the Θ/S ranges of the deep and bottom water column of the Filchner Trough during 1995, separated into western (w), central (c), and eastern (e) parts. The inset in Figure 10b indicates the appropriate areas within the Filchner Trough. The theoretical mixing lines for ISW permit identification of the source water masses whose characteristics determine the depth where melting occurs at the base of the ice shelf. In 1980, nearly 6 years before the calving event, the eastern water column is dominated by high-salinity waters from Berkner Bank (dashed line, '80e, Figure 10a). Salinities at the bottom of Filchner Trough are slightly above 34.70, consistent with measurements on the shallow areas at the ice shelf front north of Berkner Island. This is >0.05 higher than in the measurements from 1995. The western profile (dashed line, '80w) at intermediate depth (500–700 m) is influenced by Ronne waters (data points between mixing lines M_B and M_R in shaded area w, whereas the bottom waters are dominated by waters originating from Berkner Bank, shown by data points ending on mixing line M_B. At depths between 700 m and 900 m a mixed water mass (shaded area e) dominates the western part of the depression which contains waters of both sources. Hence the 1980 measurements indicate that all waters within the Filchner Trough are influenced by the Berkner source except the core of the cold ISW plume which is dominated by the Ronne source. This hydrographic structure compares well with numerical model results which depict a dominant Filchner gyre in front of the ice shelf, transporting HSSW from the Berkner Bank as well as MWDW from the north into the cavity.

In 1989, 3 years after the calving event, the HSSW source on Berkner Bank does not influence the water mass composition in the trough (Figure 10b, dashed lines '89w and '89e) because the direct inflow of HSSW from Berkner Bank into the depression is blocked. In addition, the HSSW source is shifted onto the western flank of the Berkner Bank, from where it drains under the Ronne Ice Shelf. With less dense (saline) water from the west to fill the bottom layer in the Filchner Ice Shelf cavity, an increased amount of dense and saline waters will enter the cavity from the south through the Thiel Trough [see also *Grosfeld and Gerdes*, 1998b; *Gerdes et al*., 1999]. While this is not modeled, a comparable effect can be seen in an increased anticyclonic flow along Berkner Island from the south with decreasing circulation in the central trough. The resulting change in the hydrography is reflected by the profiles from 1989 in Figure 10b, shown as dashed lines ('89e and '89w). On both sides of the depression the whole water column below 500 m depth, where the core of the ISW plume is located, is strongly dominated by Ronne Trough waters. The data points are located below the mixing line M_R, implying an initial salinity at the surface freezing point of >34.75. The higher density and depth of detachment of ISW from the ice shelf base result in ISW core temperatures less than −2.3°C.

In 1995, 9 years after the breakout, the water mass distribu-

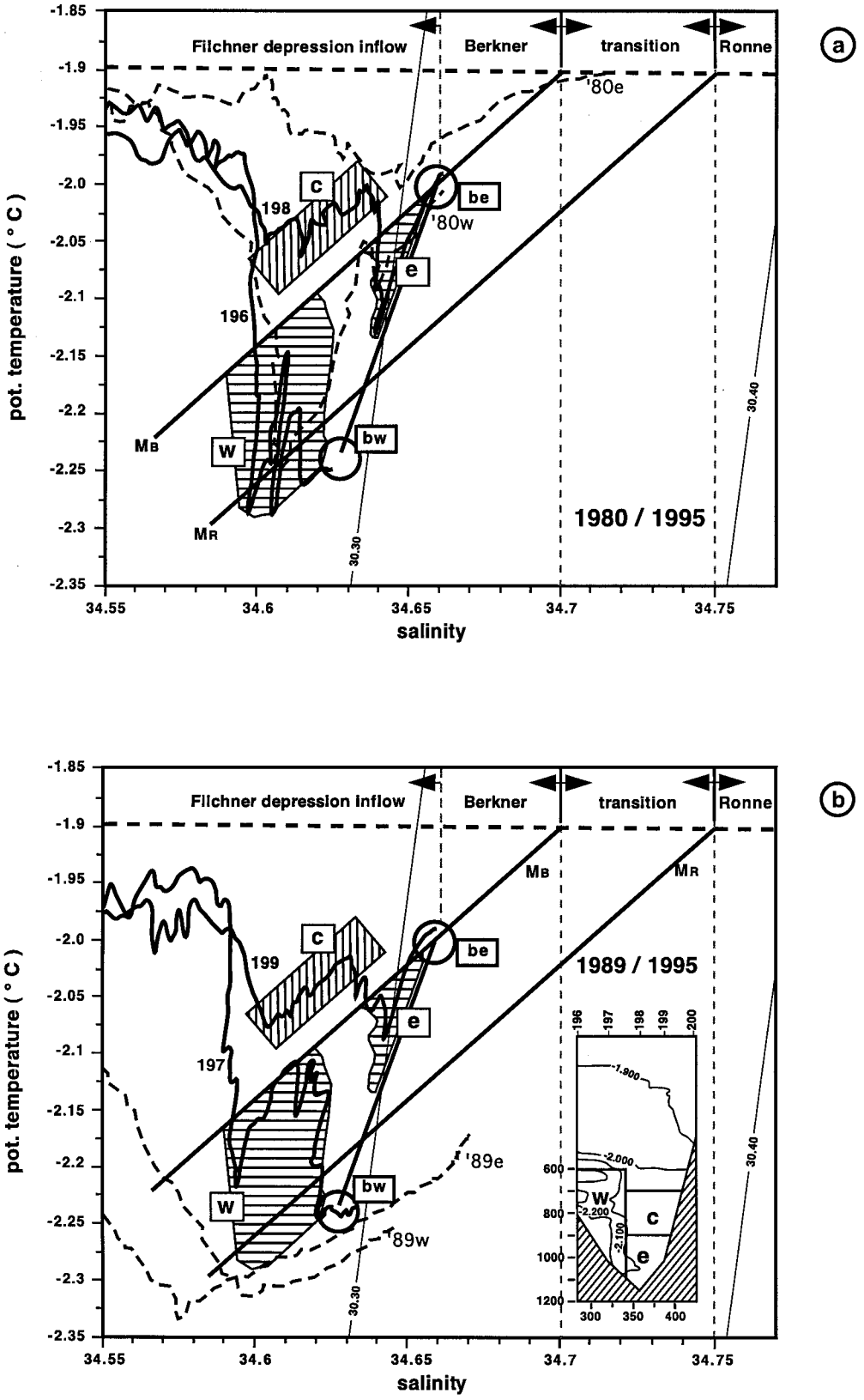

Figure 10. (a and b) Potential temperature/salinity (Θ/S) diagrams of CTD measurements for 1980 (dashed lines, '80w, station 163, and '80e, station 5) and 1989 (dashed line, '89w, station 26, and '89e, station 24), from *Nøst and Østerhus* [1998] together with measurements from 1995 (stations 196–199). The horizontal dashed line indicates the surface freezing temperature. The thick solid lines are the theoretical Θ/S correlations for ISW formed from HSSW originating on Berkner Bank (M_B) and in the Ronne Trough (M_R). Shaded areas w, c, and e correspond to depth ranges, indicated in the inset in Figure 10b. Lines for constant density are calculated at a reference pressure of 500 dbar.

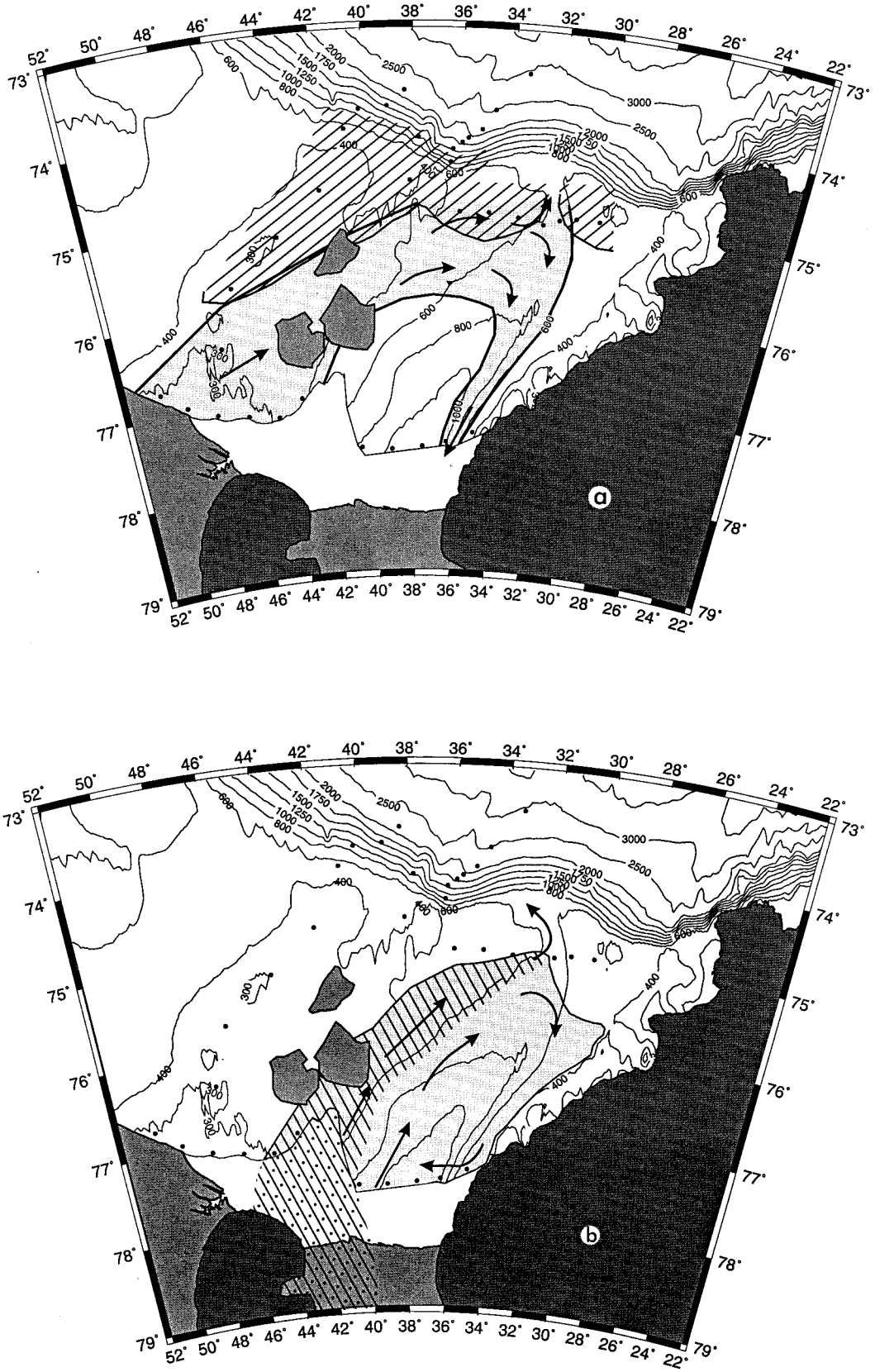

Figure 11. (a) Horizontal distribution of HSSW (shaded) and schematic representation of the flow from the shelf into the Filchner Trough (arrows). In the north the inflow of MWDW is marked (striped), and dots show 1995 station locations. (b) Horizontal distribution of the two modifications of Ice Shelf Water. The upper branch, which is able to cross the sill in the north (striped), and the lower branch, which recirculates in the depression (shaded). Also shown is the extension of the fast ice area (white area in front of the ice shelf) and the potential formation area of ice platelets (dotted lines).

tion in the Filchner Trough differs from both former conditions. In Figure 10a, station 196 on the western flank and station 198 on the central/eastern side of the deep depression are shown as thick lines, whereas stations 197 (west) and 199 (east) are plotted in Figure 10b. Bottom waters on the western side of the depression (circle b_w, $z > 800$ m) appear below the mixing line M_R and thus originate from Ronne source waters, albeit less saline and dense than in 1989. The ISW core of station 196 has a distinct component of Ronne water (Figure 10a, shaded area w) in contrast to station 197 (Figure 10b) only 25 km to the east, where less Ronne waters are evident from the location of this profile close to mixing line M_B. Mixing with recirculating waters from the central depression (shaded area c) is responsible for higher temperatures in the depth range between 700 and 850 m on station 197.

The location and slope of the central part of the profiles 198 and 199 (shaded area c) could suggest a source on Berkner Bank that takes a subsequent southerly course along the western side of Berkner Island, but that would not fit the robust cyclonic flow regime in the Filchner Trough in all scenarios. A southward flow in the central and eastern branch of the trough and a northward flow in the western branch seems more likely. The water mass at c therefore indicates a recirculation of ISW in the east of the trough, emanating from the cavity in the west which is newly ventilated with HSSW from the Berkner Bank, rather than a direct outflow out of the cavity.

On the east side of the depression (station 199), nearly the whole water column, especially the central part (shaded area c, $z > 700$ m) and the bottom waters (circle b_e, $z > 1000$ m), is controlled by water from Berkner Bank. Only waters of the eastern ISW core in the depth range 900–1000 m have a small Ronne component, resulting in a position between the mixing lines (shaded area e). Mixing causes the profile to follow the line connecting the western and eastern bottom waters b_w to b_e.

The 1995 measurements show a system shifting back to the precalving state, with only the western Filchner Trough bottom waters (station 196) showing clear Ronne characteristics. Interaction between the Berkner and Ronne source is indicated by the interleaving structures in the profile of station 196 between M_B and M_R. Modeling results also show that HSSW from the Berkner Bank slowly floods into the Filchner Trough and the circulation widens again over the whole trough after iceberg A24 has left the trough and A22 and A23 have stepped to the north or broken into pieces. We expect the influence of HSSW to increase and the bottom waters of the western branch to evolve along the mixing line from b_w to b_e to Berkner water characteristics as the remaining icebergs leave Berkner Bank.

A schematic diagram of HSSW and ISW spreading for recent conditions, derived from the model results and 1995 hydrographic measurements, is shown in Figure 11. MWDW and HSSW are mainly fed from the north into the water mass formation areas in the vicinity of the ice shelf front and into the subice cavity. HSSW originating on the shallow Berkner Bank and the area near the ice shelf front is transported toward the continental shelf break in 1995, where it partly feeds the overflow into the deep Weddell Abyssal Plain and partly recirculates near bottom southward into the cavity (Figure 11a). ISW from the subice cavity is also transported toward the sill, following the large-scale flow pattern (Figure 11b). The lower ISW core (light shading) mostly recirculates within the depression due to its higher density. The upper ISW (dashed range) overrides the HSSW water mass at the sill and also leaves the system into the deep Weddell Abyssal Plain. When emerging from the ice shelf cavity, the upper ISW core rises and releases ice platelets, which form a thick fast ice tongue in front of the ice shelf (dotted area). En route northward the upper ISW mixes with HSSW by freshening and cooling Berkner Bank source waters, influencing outflows into the deep Weddell Abyssal Plain.

Because the model is closed at the northern boundary and prescribed with fixed Θ-S values, it reveals smaller changes than the observations. Station 143 of the 1995 measurements at the continental slope to the Weddell Abyssal Plain (compare with Figure 3), in the center of the overflowing ISW plume, shows significantly warmer (-1.692°C instead of -1.93°C) and slightly saltier (34.628 instead of <34.62) values than reported by *Foldvik et al.* [1985b] for conditions before the calving event.

6. Summary and Conclusion

In 1986, three giant icebergs calved from the Filchner Ice Shelf front and subsequently grounded on the Berkner Bank. A combination of model experiments and hydrographic measurements was used to investigate the effect of these events on the oceanic circulation and water mass transformation in that region. The grounding changed the circulation pattern in the Filchner Trough, cutting off the region from its normal HSSW source, reducing thermohaline ventilation of the Filchner Ice Shelf cavity and its ISW outflow. Consequently, the net basal mass loss (comprising melting minus freezing) in the deep ice shelf cavity (areas >100 km distant from the ice shelf edge) decreases for >10%, i.e., from 19.4 to 17.2 Gt yr^{-1}, while melting in the near ice edge region increases due to the increased draft of the ice shelf edge from 5.9 to 7.1 Gt yr^{-1}. Although the total net basal melting for the whole ice shelf area did not alter significantly (from 25.3 to 24.3 Gt yr^{-1}), the changed circulation has still great influence on the water mass formation in the Filchner Trough. The physical barrier aspect of the iceberg grounding is therefore of greater importance for the local water mass modification than the role of icebergs as a freshwater source.

The combination of model results and field data leads to the following synthesis for the impact of iceberg calving in the Filchner Trough confirming hydrographic studies by *Nøst and Østerhus* [1998] for the period from 1986 until 1989.

1. Precalving, water characteristics in the deep trough are dominated by HSSW originating on the shallow Berkner Bank. Dense waters drain with the main circulation from the shallow bank into the trough and fill the bottom layers. ISW outflow in the medium depth range along the western flank is a mixture of waters from Berkner Bank and Ronne Trough. The inflow in the east consists of a mixture of HSSW from Berkner Bank and recirculating ISW.

2. Shortly after the calving, grounding of the icebergs on Berkner Bank shifts HSSW formation to the area west of the icebergs and reduces the transport of the Filchner gyre. Circulation from the north into the ice shelf cavity diminishes but is compensated by an enhanced inflow from the south, which replaces dense bottom layers in the southern part of the cavity by HSSW formed in the Ronne Trough.

3. Postcalving, as iceberg A24 left the trough and A22 and A23 shifted northward, the HSSW source on Berkner Bank regains its precalving influence. Near bottom, the western outflow of ISW maintains a clear Ronne Trough signal. Exiting

the cavity, ISW mixes with HSSW from the Berkner Bank, partly recirculates on the eastern side of the trough at a shallower depth, and overrides undiluted HSSW which enters the cavity from the north. Except for the western outflow, Berkner Bank waters dominate the water column.

While the icebergs were grounded on Berkner Bank, some HSSW formed in that area took a northward path around the iceberg positions. Reaching the sill, it split into two branches, one merging with the northward flowing shallow ISW core from the ice shelf cavity and feeding into the overflow, which forms Weddell Sea Bottom Water. The temperature of that mixture was significantly warmer and slightly saltier than reported prior to the calving event. The other branch of HSSW recirculated in the trough and participated in the ventilation of the ice shelf cavity.

In October 1998, another large iceberg (A38 at 5250 km^2) calved from the eastern Ronne Ice Shelf front, west of Berkner Island. Because of its lesser draft (~200–300 m) and the increasing bathymetric depth west of Berkner Bank it did not ground but tracked northwest with the general oceanic circulation on the shelf. This calving event was unable to obstruct the local circulation or to significantly impact the water masses and circulation, but the 30 km retreat of the ice shelf front effectively increases the water column depth beneath the new ice shelf front. This might lead to a better ventilation of the Ronne Ice Shelf cavity with increased HSSW drainage from the Berkner Bank, a "spin-up" of the anticyclonic flow around Berkner Island, and enhanced ventilation of the Filchner Ice Shelf cavity, increasing ISW production and outflow.

Acknowledgments. We are grateful to Master Jonas with the officers and crew of *Polarstern* as well as the members of the mooring and the CTD groups on board cruise ANT XII/3. The computations were carried out at the computing center of the Alfred-Wegener-Institut and the German Climate Computer Center (DKRZ) at Hamburg. We thank the anonymous reviewers and especially S. Jacobs for helpful comments and suggestions. This work was partly funded by the German CLIVAR-Project, contract 03FO246F3.

References

Beckmann, A., H. H. Hellmer, and R. Timmermann, A numerical model of the Weddell Sea: Large-scale circulation and water mass distribution, *J. Geophys. Res*., *104*, 23,375–23,391, 1999.

Bryan, K., A numerical method for the study of the circulation of the world ocean, *J. Comput. Phys*., *4*, 347–376, 1969.

Carmack, E. D., and T. D. Foster, Circulation and distribution of oceanographic properties near the Filchner Ice Shelf, *Deep Sea Res*., *22*, 77–90, 1975.

Cox, M. D., A primitive equation, 3-dimensional model of the ocean, *GFDL Ocean Group Tech. Rep. 1*, Geophys. Fluid Dyn. Lab., Princeton Univ., Princeton, N. J., 1984.

Dieckmann, G., G. Rohardt, H. H. Hellmer, and J. Kipfstuhl, The occurence of ice platelets at 250 m depth near the Filchner Ice Shelf and the significance for sea ice biology, *Deep Sea Res*., *33*, 141–148, 1986.

Engelhardt, H., and J. Determann, Borehole evidence for a thick layer of basal ice in the central Ronne Ice Shelf, *Nature*, *327*, 318–319, 1987.

Fahrbach, E., R. G. Peterson, G. Rohardt, P. Schlosser, and R. Bayer, Suppression of bottom water formation in the southeastern Weddell Sea, *Deep Sea Res*., *Part I*, *41*, 389–411, 1994.

Ferrigno, J. G., and W. G. Gould, Substantial changes in the coastline of Antarctica revealed by satellite imagery, *Polar Rec*., *23*, 577–583, 1987.

Foldvik, A., and T. Gammelsrød, Notes on Southern Ocean hydrography, sea ice and bottom water formation, *Palaeogeogr. Palaeoclimatol. Palaeoecol*., *67*, 3–17, 1988.

Foldvik, A., T. Gammelsrød, and T. Tørresen, Circulation and water masses on the southern Weddell Sea shelf, in *Oceanology of the Antarctic Continental Shelf*, *Antarct. Res. Ser*., vol. 43, edited by S. Jacobs, pp. 5–20, AGU, Washington, D. C., 1985a.

Foldvik, A., T. Gammelsrød, and T. Tørresen, Physical oceanography studies in the Weddell Sea during the Norwegian Antarctic Research Expedition 1978/79, *Polar Res*., *3*, 195–207, 1985b.

Foster, T. D., and E. C. Carmack, Frontal zone mixing and Antarctic Bottom Water formation in the southern Weddell Sea, *Deep Sea Res*., *23*, 301–317, 1976.

Fox, A., and A. P. R. Cooper, Measured properties of the Antarctic Ice Sheet derived from SCAR Antarctic digital database, *Polar Rec*., *30*, 201–206, 1994.

Gade, H. G., Melting of ice in sea water: A primitive model with application to the Antarctic ice shelf and icebergs, *J. Phys. Oceanogr*., *9*, 189–198, 1979.

Gammelsrød, T., and N. Slotsvik, Hydrographic and current measurements in the southern Weddell Sea 1979/80, *Polarforschung*, *51*, 101–111, 1981.

Gammelsrød, T., L. F. Anderson, E. Fogelkvist, A. Foldvik, E. P. Jones, O. A. Nøst, K. Olsson, Ø. Skagseth, T. Tanhua, and S. Østerhus, Distribution of water masses on the continental shelf in the southern Weddell Sea, in *The Polar Oceans and Their Role in Shaping the Global Environment*, *The Nansen Centennial Volume*, *Geophys. Monogr. Ser*., vol. 84, edited by M. Johannessen, R. D. Muench, and J. E. Overland, pp. 159–175, AGU, Washington, D. C., 1994.

Gerdes, R., A primitive equation ocean circulation model using a general vertical transformation, part 1, Description and testing of the model, *J. Geophys. Res*., *98*, 14,683–14,701, 1993.

Gerdes, R., J. Determann, and K. Grosfeld, Ocean circulation beneath Filchner-Ronne Ice Shelf from three-dimensional model results, *J. Geophys. Res*., *104*, 15,827–15,842, 1999.

Gordon, A. L., Oceanography of Antarctic Waters, in *Antarctic Oceanology I*, *Antarct. Res. Ser*., vol. 15, edited by J. L. Reid, pp. 169–203, 1971.

Grosfeld, K., Untersuchungen zu Temperaturregime und Massenhaushalt des Filchner-Ronne-Schelfeises, Antarktis, unter besonderer Berücksichtigung von Anfrier-und Abschmelzprozessen, *Rep. Polar Res*., *130*, 148 pp., 1993.

Grosfeld, K., and R. Gerdes, Circulation beneath the Filchner Ice Shelf and its sensitivity to changes in the oceanic environment: A case study, *Ann. Glaciol*., *27*, 99–104, 1998a.

Grosfeld, K., and R. Gerdes, Circulation in the Filchner-Ronne Ice Shelf Domain: First results from a 3D-Ocean Model, in *Filchner-Ronne Ice Shelf Rep. 12*, pp. 35–39, Alfred-Wegener Inst. for Polar and Mar. Res., Bremerhaven, Germany, 1998b.

Grosfeld, K., R. Gerdes, and J. Determann, Thermohaline circulation and interaction beneath ice shelf cavities and the adjacent open ocean, *J. Geophys. Res*., *102*, 15,595–15,610, 1997.

Grosfeld, K., H. H. Hellmer, M. Jonas, H. Sandhäger, M. Schulte, and D. G. Vaughan, Marine ice beneath Filchner Ice Shelf: Evidence from a multidisciplinary approach, in *Ocean, Ice and Atmosphere: Interactions at the Antarctic Continental Margin*, *Antarc. Res. Ser*., vol. 75, edited by S. Jacobs and R. Weiss, pp. 319–339, AGU, Washington, D. C., 1998.

Harms, S., E. Fahrbach, and V. H. Strass, Sea ice transports in the Weddell Sea, *J. Geophys. Res*., in press, 2001.

Jacobs, S. S., H. H. Hellmer, C. S. M. Doake, A. Jenkins, and R. M. Frolich, Melting of ice shelves and mass balance of Antarctica, *J. Glaciol*., *38*, 375–386, 1992.

Kottmeier, C., and L. Sellmann, Atmospheric and oceanic forcing of Weddell Sea ice motion, *J. Geophys. Res*., *101*, 20,809–20,824, 1996.

Lewis, E. L., and R. G. Perkin, Ice pumps and their rates, *J. Geophys. Res*., *91*, 11,756–11,762, 1986.

Lusquinos, A., Extreme temperatures in the Weddell Sea, *Arbok Univ. Bergen Mat. Naturvitensk. Ser*., *23*, 19 pp., 1963.

Markus, T., The effect of the grounded tabular icebergs in front of the Berkner Island on the Weddell Sea ice drift as seen from satellite passive microwave sensors, in *IGARSS '96: Remote sensing for a sustainable future*, pp. 1791–1793, IEEE Press, Piscataway, N.J., 1996.

Melles, M., G. Kuhn, D. K. Fütterer, and D. Meischner, Processes of modern sedimentation in the southern Weddell Sea, Antarctica—Evidence from surface sedimentation, *Polarforschung*, *64*(2), 45–74, 1994.

Nøst, O. A., and A. Foldvik, A model of ice shelf-ocean interaction

with application to the Filchner-Ronne and the Ross Ice shelves, *J. Geophys. Res*., *99*, 14,243–14,254, 1994.

Nøst, O. A., and S. Østerhus, Impact of grounded icebergs on the hydrographic conditions near the Filchner Ice Shelf, Antarctica, in *Ocean, Ice and Atmosphere: Interactions at the Antarctic Continental Margin*, *Antarct. Res. Ser*., vol. 75, edited by S. Jacobs and R. Weiss, pp. 269–286, AGU, Washington, D. C., 1998.

Oerter, H., J. Kipfstuhl, J. Determann, H. Miller, D. Wagenbach, A. Minikin, and W. Graf, Evidence for basal marine ice in the Filchner-Ronne Ice Shelf, *Nature*, *358*, 399–401, 1992.

Reid, J. L., and R. L. Lynn, On the influence of the Norwegian-Greenland and Weddell Sea upon the bottom waters of the Indian and Pacific oceans, *Deep Sea Res*., *18*, 1063–1088, 1971.

Robin, G. de Q., Formation, flow and disintegration of ice shelves, *J. Glaciol*., *24*, 259–271, 1979.

Rohardt, G., Hydrographische Untersuchungen am Rande des Filchner Schelfeises, *Rep. Polar Res*., *19*, 137–143, 1984.

Schenke, H. W., S. Dijkstra, F. Niederjasper, and T. Schöne, The new bathymetric charts of the Weddell Sea: AWI BCWS, in *Ocean, Ice and Atmosphere: Interactions at the Antarctic Continental Margin*, *Antarct. Res. Ser*., vol. 75, edited by S. Jacobs and R. Weiss, pp. 371–380, AGU, Washington, D. C., 1998.

Schlosser, P., R. Bayer, A. Foldvik, T. Gammersrød, G. Rohardt, and K. O. Münnich, Oxygen 18 and helium as tracers of ice shelf water and water/ice interaction in the Weddell Sea, *J. Geophys. Res*., *95*, 3253–3263, 1990.

Schröder, M., and E. Fahrbach, On the structure and the transport in the eastern Weddell Gyre, *Deep Sea Res*., *Part II*, *46*, 501–527, 1999.

Schröder, M., R. Hamann, O. Klatt, E. Nygaard, E. Schütt, L. Sellmann, N. Steiner, V. Strass, R. Timmermann, and G. Traue, Physikalische Ozeanographie, Nährstoffe und Tracer, in *Die Expedition ANTARKTIS-XII mit FS "Polarstern", Berichte vom Fahrtabschnitt ANT-XII/3*, edited by W. Jokat and H. Oerter, *Rep. Polar Res*., *219*, 19–36, 1997.

Stevens, D. P., The open boundary condition in the United Kingdom Fine- Resolution Antarctic Model, *J. Phys. Oceanogr*., *21*, 1494–1499, 1991.

Thyssen, F., A. Bombosch, and H. Sandhäger, Elevation, ice thickness and structure mark maps of the central part of Filchner-Ronne Ice Shelf, Antarctica, *Polarforschung*, *62*, 17–26, 1992.

Vaughan, D. G., Chasing the rogue icebergs, *New Sci*., *9*, 24–27, 1993.

Vaughan, D. G., J. Sievers, C. S. M. Doake, H. Hinze, D. R. Mantripp, V. S. Pozdeev, H. Sandhäger, H. W. Schenke, A. Solheim, and F. Thyssen, Subglacial and seabed topography, ice thickness and water column thickness in the vicinity of Filchner-Ronne-Schelfeis, Antarctica, *Polarforschung*, *64*, 75–88, 1994.

Weiss, R. F., H. G. Östlund, and H. Craig, Geochemical studies of the Weddell Sea, *Deep Sea Res*., *26*, 1093–1120, 1979.

Wingham, D. J., C. S. M. Doake, D. R. Mantripp, J. Ihde, R. Scharroo, H.-W. Schenke, and J. Sievers, ESAMCA (Exploitation of satellite altimetry for the monitoring of climate-related change of Antarctic ice shelves), project final report, *DGXII Environment Programme Phase II contract EV5C-CT94-0483*, Mullard Space Sci. Lab., Holmbury St. Mary, England, 1997.

E. Fahrbach, R. Gerdes, A. Mackensen, and M. Schröder, Alfred Wegener Institute for Polar and Marine Research, Postfach 120161, Columbusstrasse, D-27515 Bremerhaven, Germany.

K. Grosfeld, Institute for Geophysics, Corrensstrasse 24, D-48149 Münster, Germany. (grosfel@uni-muenster.de)

(Received August 22, 2000; revised January 5, 2001;
accepted January 16, 2001.)